Label-free fluorescent and electrochemical biosensors based on defective G-quadruplexes

Jing Zhang, Liang-Liang Wang, Mei-Feng Hou, Li-Pei Luo, Yi-Juan Liao, Yao-Kun Xia, An Yan, Yun-Ping Weng, Lu-Peng Zeng, Jing-Hua Chen

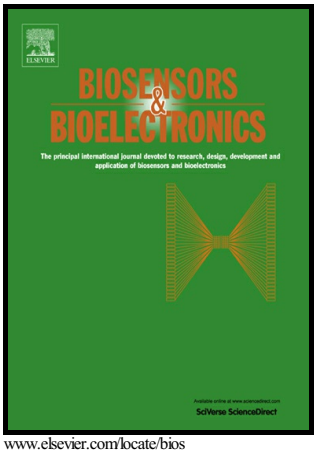

www.elsevier.com/locate/bios

PII: S0956-5663(18)30534-7
DOI: https://doi.org/10.1016/j.bios.2018.07.033
Reference: BIOS10622

To appear in: *Biosensors and Bioelectronic*

Received date: 26 April 2018
Revised date: 13 July 2018
Accepted date: 16 July 2018

Cite this article as: Jing Zhang, Liang-Liang Wang, Mei-Feng Hou, Li-Pei Luo, Yi-Juan Liao, Yao-Kun Xia, An Yan, Yun-Ping Weng, Lu-Peng Zeng and Jing-Hua Chen, Label-free fluorescent and electrochemical biosensors based on defective G-quadruplexes, *Biosensors and Bioelectronic,* https://doi.org/10.1016/j.bios.2018.07.033

Label-free fluorescent and electrochemical biosensors based on defective G-quadruplexes

Jing Zhang[a,*], Liang-Liang Wang[b], Mei-Feng Hou[a], Li-Pei Luo[b], Yi-Juan Liao[a], Yao-Kun Xia[b], An Yan[b], Yun-Ping Weng[b], Lu-Peng Zeng[b], Jing-Hua Chen[b,*]

[a] College of Life Sciences, Fujian Agriculture and Forestry University, Fuzhou, Fujian Province 350002, P R China.

[b] Department of Pharmaceutical Analysis, The School of Pharmacy, Fujian Medical University, Fuzhou, Fujian Province 350108, P. R. China.

1601225385@qq.com(J. Zhang)
cjh_huaxue@126.com (J. H. Chen)

[*]Corresponding author.

Abstract: Abnormal levels of guanine closely associated with plenty of diseases are usually used as a biomarker for clinical diagnosis. In order to detect guanine and its derivatives accurately, in this paper, a defective G-quadruplex (DGQ) containing a G-vacancy at one of its G-quartet layers, and two kinds of G-quadruplex specific indicators including thioflavine T (ThT) and hemin were used for constructing a fluorescent and an electrochemical biosensor, respectively. In brief, a G-rich DNA probe is designed to form either hairpin or DGQ structure. In the absence of guanine, G-rich probes prefer to maintain hairpin structure and nearly have no interaction with ThT or hemin, leading to almost negligible signals. Upon addition of guanine, the G-rich probe fold into DGQ structure and then the G-vacancy in it is filled up immediately by guanine via Hoogsteen hydrogen bonds, resulting canonical G-quadruplex formation. Accordingly, ThT or hemin can selectively combine with G-quadruplex, giving rise to distinct fluorescent or current signal changes for label-free detection of guanine. Benefiting from the perfect discriminative ability of guanine towards DGQ and ThT/hemin against standard G-quadruplex, the fluorescent and electrochemical biosensors present better sensitivity and selectivity for guanine

detection with the limit of detection (LOD) as low as 18.26 and 0.36 nM, respectively. Successful attempts were also made in applying the proposed electrochemical biosensor to detect guanine in drugs and urine, obtaining satisfactory recovery rates of 99 %~104 % and 96 % ~106 %, respectively.

Keywords: Defective G-quadruplex; Guanine; Thioflavine T; Hemin; Fluorescent biosensor; Electrochemical biosensor.

1. Introduction

As building blocks of nucleotides, guanine is a vital element in the coding of genetic information and plays a crucial role in numerous biological processes (Neves et al., 2002; Niu et al., 2012). Recently, it is reported the abnormal concentrations of guanine and its derivatives were capable of manifesting metabolic disorders and a variety of diseases in human body, such as cancer (Chabosseau et al., 2011), aging (Burhans and Weinberger, 2007), kidney diseases (Kimura et al., 2003), gout (Boss and Seegmiller, 1982) , and a few of mitochondrial pathologies (Pitceathly et al., 2012). Therefore, the detection of guanine and its derivatives is important and meaningful (Jordheim et al., 2013).

So far, different methods for the detection of guanine and its derivatives have been widely reported, including capillary electrophoresis (CE) (Chen et al., 2002), liquid chromatography-mass spectrometry (LC-MS) (Fan et al., 2006), capillary

electrophoresis-mass spectrometry (CE-MS) (Cahours et al., 2000) and so on. However, these methods either possess relatively low sensitivity or require complicated apparatus and high cost. Notably, due to known merits and considerable prospect (Shen and Xia, 2014; Wu et al., 2014), some fluorescent sensing strategies were applied to detect guanine and its derivatives (Cui et al., 2014; Li et al., 2012; Lu et al., 2016; Pang et al., 2016; Yoshimoto et al., 2003). Tan's group proposed a special defective G-quadruplex (DGQ) with ultrahigh discriminative ability against guanine (Li et al., 2015). In general, the standard canonical G-quadruplex is composed of three consensus intact G-quartet layers. In each layer, four guanine bases associate with each other through eight Hoogsteen hydrogen bonds (Biffi et al., 2013; Burge et al., 2006; Zhu et al., 2015). Differently, DGQ consists of three G3 and one G2 tracts, that is, there is a G-vacancy at one corner of its G-quartet layers (Scheme 1B). Just due to such vacancy having particular requirements for Hoogsteen hydrogen bonds and planar structure to change into canonical G-quadruplex, DGQ possesses exceptional selectivity for guanine recognition. That is, only guanine and its derivatives can fill up this vacancy and fulfill the conversion from incomplete G-quadruplex to intact one. Based on this unordinary DNA structure, Tan's group established a labeled sensing strategy for ultrasensitive detection of guanine and its derivatives, in which polyethylene glycol (PEG200) was used as a crowding reagent

to promote standard G-quadruplex formation (Li et al., 2016). However, PEG is non-specific to G-quadruplex, in other words, it also facilitates the DGQ formation in the absence of guanine, generating large background signals (Kan et al., 2006). Moreover, the labeling of the fluorescent dye and quencher makes the assay cost-, time- and labor-consuming. To overcome the above limitations, a label-free strategy using a G-quadruplex specific promoter for DGQ-to-G-quadruplex conversion is worth to be expected.

Surprisingly, Mohanty et al. and Sugimoto et al. proposed a G-quadruplex specific fluorescent indicator, named Thioflavin T (ThT) (Mohanty et al., 2013; Sugimoto et al., 2015). This water-soluble fluorescent dye itself bears extremely low fluorescence, while it exhibits great fluorescence enhancement if and only if it combines with G-quadruplex DNA under physiological salt conditions. That is to say, other DNA forms including single-strand and duplexes can't drive such a change. Tan et al. and our group have reported two kinds of fluorescent biosensors based on ThT-induced G-quadruplex formation for biomolecules detection (Chen et al., 2014; Tan et al., 2014). Additionally, it is worth noting that hemin is also a G-quadruplex specific substance. It can impel G-rich nucleic acids to fold into G-quadruplex DNA structure and then combine with it to constitute stable G-quadruplex-hemin complex in the presence of a metal ion, such as K^+ (Marchand and Gabelica, 2016). This complex,

called DNAzyme, has horseradish peroxidase-like activity and can effectively catalyze the H_2O_2-mediated oxidation along with the change of current signals and the color in reaction solution (Chen et al., 2018; Li et al., 2009). Note that only G-quadruplex has this kind of especial property, instead of all other DNA structures. Moreover, G-quadruplex-hemin DNAzyme is of better stability and lower cost when compared to other DNAzymes and proteases (Ito and Hasuda, 2004; Willner et al., 2008). Gao et al. and our group have utilized the unique characteristic of hemin specific to G-quadruplex to establish label-free electrochemical biosensor for DNA or microRNA detection (Gao et al., 2017; Zhang et al., 2014).

In order to increase assay sensitivity, reduce testing costs and simplify the procedures for guanine and its derivatives detection, we herein develop two varieties of label-free biosensors by coupling DGQ with ThT (for fluorescent sensor) or hemin (for electrochemical sensor). As illustrated schematically in scheme 1 and 2, a G-rich DNA probe is designed to form either hairpin (H1 or H3) or DGQ structure containing a G-vacancy at one corner of its G-quartet layers. Initially, the probe prefers to maintain hairpin structure in the absence of free guanines. Owing to the perfect discriminative ability of ThT and hemin towards intact G-quadruplex instead of hairpin, the fluorescent and electrochemical signals are nearly negligible. Whereas, upon the addition of guanine, the G-rich probe turns into DGQ structure and then its

G-vacancy is filled up immediately by guanine to form stable standard G-quadruplex, which subsequently combines with ThT or hemin leading to a dramatic increase of fluorescent or electrochemical signals. By monitoring the signal differences before and after guanine addition, the proposed biosensors can sense the existence and precise quantity of guanine with ultrahigh sensitivity and selectivity. Particularly, together with the intrinsically electrochemical advantages of short analysis time, simple operation, low cost, high sensitivity and so on, the label-free electrochemical sensor holds great potential application in point-of-care testing (POCT).

2 Experimental sections

2.1. Reagents and apparatus

All oligonucleotides (fluorescent DNA probes: H1: 5'-TAGGGTGGGCTGGGAGGTTTTTTTTTTCACCCTA-3', H2: 5'-FAM-TAGGGTGGGCTGGGAGGTTTTTTTTTTCACCCTA-BHQ1-3'; electrochemical DNA probes: H3: 5'-TAGGGTGGGCTGGGAGGTTTTTTTTTTCACCCTA-SH-3', H4: 5'-MB-TAGGGTGGGCTGGGAGGTTTTTTTTTTCACCCTA-SH-3'. FAM, BHQ1 and MB represent Carboxyfluorescein, black hole quencher 1 and methylene blue, respectively) were synthesized by Sangon Biotech (Shanghai, China) Co., Ltd, and purified by high performance liquid chromatography (HPLC) then confirmed by mass spectrometry (MS). The concentrations were quantified by OD260 (optical density at 260 nm using standard cuvette with 1 cm optical distance.) based on their individual absorption coefficients. H1 was prepared by 50 mM Tris-HCl (pH 7.2) including 10 mM KCl and 10 mM $MgCl_2$. H2 was prepared according to the relevant

reference (Li et al., 2016). H3 and H4 were dissolved in the 10 mM TE buffer (Tris and EDTA, pH 7.2) consisting of 10 mM trichloroethyl phosphate (TCEP) and 1 M NaCl. ThT, hemin, H_2O_2, 3, 3', 5, 5'-tetramethylbenzidine (TMB) and other chemical reagents were all purchased from Sigma-Aldrich. ThT was dissolved in 50 mM Tris-HCl. The stock solution of hemin was prepared in dimethylsulfoxide (DMSO), stored in the dark at -20 ℃ and diluted to the required concentration with 10 mM TE buffer solution. All other chemicals were of analytical grade and all aqueous solutions were prepared with Milli-Q water (18.2 MΩ/cm).

2.2. Experimental protocols

The circular dichroism (CD) measurements: The CD spectra were resolved by the Jasco J-810 circular dichroism spectropolarimeter (Tokyo, Japan). The optical chamber was deoxygenated with dry purified nitrogen (99.99 %) prior to use and kept under a nitrogen atmosphere during the experiments. The spectra were measured using a quartz cuvette with 1.0 cm path length and 1s response time. Each spectrum subtracted the background of the buffer solution was an average of three repetitive measurements at 25 °C.

Fluorescence measurements: After different concentrations of guanine were added and mixed thoroughly, the sample solutions were incubated at room temperature and then transferred to quartz fluorescent cuvettes (4 mm × 10 mm, Sub-micro, 50 μL) for detection by an F-4600 fluorescence spectrophotometer (HITACHI, Japan). The fluorescence spectra of the above solutions were recorded in different wavelength (excitation and emission wavelength were 441 and 485 nm for H1, 488 and 520 nm for H2, respectively) at room temperature with 5 nm slit and 650 V detector voltage of photoelectric multiplier (PMT).

UV-Vis measurements: The UV-Vis absorbance spectra were recorded by UV-2450 spectrophotometer (Shimadzu, Japan) with 1.0 cm optical pathway from 350 to 500 nm.

Electrochemical measurements: All electrochemical measurements were carried out on CHI 660E electrochemical workstation (CH Instrument, Shanghai, China), including a working electrode (a gold electrode, 2 mm diameter), a platinum wire as the counter electrode, and a reference electrode (Ag/AgCl, 3 M KCl). Before the fabrication process of the biosensor, the gold electrodes were firstly polished on microcloth with 0.05 and 0.3 μm alumina powder to obtain mirror surface. After cleaned with ethanol and Milli-Q water for 5 min, respectively, these electrodes were electrochemically treated to remove any remaining impurities (Hoogvliet et al., 2000) until the steady state of current curve in 0.5 M H_2SO_4 solution was reached (Fan et al., 2003). Subsequently, the electrochemical G-rich probe (H3 or H4) was immobilized on the resulted electrodes for 1 hour, followed by the blocking effect of 1 mM MCH for 2 hour to preclude the nonspecific adsorption. Then the probe-modified electrodes were measured with various electrochemical methods. Cyclic voltammetry (CV) was performed at a scan rate of 100 mV/s in the potential range of -0.20 V~+0.80 V. Chronoamperometry was recorded within 100 s. Differential Pulse Voltammetry (DPV) was measured within a potential range of -0.35 V~0.00 V, a sampling rate of 0.0167 s, a pulse width of 0.05 s and an amplitude of 0.05 V.

3. Results and discussion

3.1. Experimental principle of the label-free fluorescent biosensor

As illustrated in Scheme 1, the fluorescent G-rich probe H1 is devised to exist in either hairpin or DGQ form. In the absence of guanine, H1 prefers to fold into hairpin

structure via self-hybridization of the nucleotides near the two ends. On account of little response to hairpin DNA, ThT shows very weak fluorescence. With guanine addition, the probe convert to an intact G-quadruplex since guanine fills the G-vacancy in its G-quartet layers through Hoogsteen hydrogen bonds. Meanwhile, ThT specifically binds the special site (Mohanty et al., 2013) in G-quadruplex, leading to conspicuous enhancement of fluorescence to sense the existence and exact amount of guanine.

3.2. The feasibility of the label-free fluorescent biosensor

In order to verify the feasibility of the proposed biosensor, fluorescence spectra of ThT and H1 before and after guanine addition were firstly recorded. As depicted in Figure 1A, ThT solution (curve a) shows negligible fluorescent intensity after the addition of H1 (curve b) and further addition of K^+ (curve c), while a prominent enhancement upon guanine injection (curve d). This obvious rise indicates the ultra-high discriminating ability of ThT to G-quadruplex as well as the satisfactory signal-to-noise. Then, the CD spectra of H1 in different solutions were characterized to investigate the overall process of the proposed fluorescent biosensor. As shown in Figure 1B, there are a tiny positive peak at around 265 nm and a negative peak near 245 nm (curve a) for H1 and K^+ mixture, indicating the existence of base stacking and helicity (Balagurumoorthy and Brahmachari, 1994; Zhang et al., 2014). Here, H1 favors to keep in hairpin form. In the absence of guanine, ThT only gives rise to a negligible change on both positive and negative peak (curve b), indicating weak effects of ThT against hairpin structure of H1 as well as very low background signals. When guanine is added into H1 and K^+ mixture, the positive and negative peaks become a little bit higher and deeper, respectively (curve c), confirming the formation

of stable definite parallel G-quadruplex (Li et al., 2015; Marck and Thiele, 1978). With the addition of ThT into the above resulted solution, the peaks value increase further (curve d), which demonstrates the function of ThT as a G-quadruplex inducer. All these data descript the transition from hairpin to G-quadruplex clearly during the whole fabrication of this biosensor along with the high selectivity of ThT for G-quadruplex. Subsequently, we also used UV-Vis spectra to further validate the feasibility of the fluorescent biosensor. As shown in Figure 1C, ThT exhibits its representatively maximum absorption profile at 413 nm (curve a). After addition of H1 (curve b) and further addition of K^+ (curve c), the absorption peak decreases a little due to the electrostatic interaction between ThT and H1 (Balagurumoorthy and Brahmachari, 1994). In the first three steps, the absorption curve maintains almost the same maximum absorption wavelength, manifesting the similar form of H1 as hairpin structure. Whereas, upon guanine addition, conspicuous red shift from 413 to 442 nm was observed since hairpin H1 change into complete parallel G-quadruplex structure after the G-vacancy was filled up by guanine (curve d). Summarily, the UV-Vis results are in a good agreement with the aforementioned results.

3.3. Optimizations of experimental parameters

The influence of the concentration of DNA (H1), ThT, K^+ and the incubation time on the change of fluorescent intensity (ΔF) before and after the guanine addition was orderly investigated to realize the optimal properties of the label-free fluorescent biosensor. As shown in Figure S1A, ΔF soars up and subsequently decrease with the increase of the H1 concentration in the range of 1~30 μM. The optimal concentration of H1 corresponding to the maximum ΔF is 5 μM H1. In Figure S1B, ΔF enhances

quickly with the increment of ThT concentration and then reaches to a platform when the concentration is higher than 10 μM. Therefore, 10 μM ThT was selected for further use. Additionally, from Figure S1C and Figure S1D, the optimal concentration of K^+ and incubation time was obtained as 10 mM and 20 min, respectively.

3.4. Properties analysis of the label-free fluorescent biosensor

To investigate the sensitivity of this biosensor, the fluorescence intensity (F) of ThT-H1-K^+ solution with different concentrations of guanine (C) addition were measured under the optimal experimental conditions. Figure 2A shows F increased with the rising of C ranging from 50 nM to 50 μM, illustrating that more guanine added, more intact and stabilized G-quadruplex formed. Additionally, it can be observed that there is a good linear relation between ΔF and C in Figure 2A inset. The linear regression equation was described as $\Delta F=13.8789+3.3492C$ ($r=0.9952$) with the LOD of 18.26 nM, where r is the regression coefficient. Meanwhile, in order to demonstrate the better performance of the prepared label-free sensor, a similar labeled fluorescent biosensor (Figure 2C Inset) was constructed according to the relevant reference by modifying the 3' and 5' terminal of H1 with BHQ1 and FAM respectively named H2 (Li et al., 2016). In this sensor, the guanine induced DGQ-to-quadruplex structural conversion gives rise to the distance change between the fluorescent dye and the quencher labeled at the each end of the probe, together with the fluorescent signal change for guanine detection. The labeled biosensor was used to

assay guanine concentration ranging from 100 nM to 20 μM with the LOD of 45 nM (Figure S2 A), which is poorer than our proposed label-free sensor because the intermolecular fluorescent quenching and the interference of G-quadruplex formation caused by the modified moieties may lead to higher background signal as well as lower sensitivity. Furthermore, this label-free fluorescent biosensor exhibited better stability with fluorescence signal reduced less than 8 % in 72 hours.

Afterwards, we investigated the selectivity of the biosensor by comparing F increasement after addition of guanine and other analogues including UTP, CTP, ATP, inosine, xanthosine, GTP, GDP and GMP. As shown in Figure 2B, the strongest F of guanine (curve k) remarkably distinguishes from that of other analogues (curve b-j) and the blank (curve a), indicating ultrahigh selectivity of this biosensor. Although the structures of GMP, GDP, GTP (Figure S3 b) consist of guanine base, their F values are far less than that of guanine because their intrinsic negative charges produce electrostatic repulsion in the assembly process of Hoogsteen hydrogen bonds. Furthermore, the higher negative charges they bear, the stronger electrostatic repulsion they will cause along with the less F value compared to the neutral guanine (Figure S3 a). The structures of inosine and xanthosine (Figure S3 c) have the same central structures with guanine while different substituent atoms on C_2, which hinder the formation of one Hoogsteen hydrogen bond, immensely decreasing the fluorescent

signal. UTP, CTP and ATP with obvious different structures compared with guanine (Figure S3 d), are unable to formed Hoogsteen hydrogen bonds in alike manner, showing the lowest F. Above results indicate the excellent selectivity of the fluorescent biosensor. In addition, in order to quantitatively compare the recognition ability of the proposed label-free and the similar labeled (Figure S2 B) fluorescent biosensor, we defined a discrimination factor (DF) as the ratio of net F signal (ΔF, the peak value of target minus the background) obtained with guanine to that produced by the analogues. Figure 2C shows obviously, the label-free biosensor bears better identification ability toward guanine because the high specificity of ThT as well as the elimination of the intermolecular fluorescent quenching caused by the labeled strategy.

In summary, the label-free fluorescent biosensor exhibited superior sensitivity compared with the most existing methods (Table S1) and excellent selectivity due to the recognizable ability of ThT to G-quadruplex and guanine to DGQ structure. Whereas, it is difficult to meet the requirement of POCT for disease screenings or prognosis monitoring purpose, such as ultra-sensitive, affordable, potable and so on (Topkaya et al., 2016). Note that electrochemical biosensors have considerable advantages of outstanding sensitivity, rapid response, low cost and portability, and have been shown to offer good performance in sensitive and specific analysis of

biomolecules (Labib et al., 2016). All above merits make electrochemical biosensors a promising alternative for POCT. Therefore, based on the label-free fluorescent biosensor, we introduced hemin as another specific indicator for standard G-quadruplex recognition to constitute a label-free electrochemical biosensor as illustrated in next section, and then employed it to measure the guanine concentration in drug and urine.

3.5. Experimental principle of the label-free electrochemical biosensor

Accordingly, we subsequently constitute a label-free electrochemical biosensor combined with horseradish peroxidase-like activity generated by G-quadruplex-hemin DNAzyme. As it shown in Scheme 2A, the G-rich probe H3 similar to H1 also having either hairpin or DGQ form is immobilized on the gold electrode surface via Au-S bond. In the absence of guanine, the H3 modified electrode exhibits extremely poor current signal when immersed into H_2O_2/TMB solution including hemin and K^+ due to no interaction between the hairpin H3 and hemin. In the presence of guanine, it confers the conversion of H3 from hairpin to stable G-quadruplex by filling G-vacancy. As a result, hemin selectively binds with the G-quadruplex to form G-quadruplex-hemin DNAzyme, yielding great current enhancement of H_2O_2/TMB solution as well as a color change from colorless to blue for guanine detection.

3.6. The feasibility of the label-free electrochemical biosensor

Cyclic voltammograms were adopted to study the feasibility of this electrochemical biosensor. As shown in Scheme 2B, there are two pairs of redox peaks (curve a) when the H3 modified gold electrode is immersed into H_2O_2/TMB solution in the presence of K^+. With addition of guanine (curve c) or hemin(curve d), the curves show little change in comparison with the former one (curve a). Furthermore, there also exhibits two pairs of redox peaks similar to curve a when the bare gold electrode is immersed into H_2O_2/TMB solution in the presence of K^+ and hemin (curve b), indicating hemin itself has poor catalytic activity. However, in the coexistence of hemin, guanine and K^+ (curve e), the H3 modified electrode displays a dramatically increase in the reduction peak accompanied by a color change from colorless to blue (inset e), accounting for the catalytic activity of G-quadruplex-hemin DNAzyme. Meanwhile, the CD spectrum (Figure S4) was also used to characterize the whole transition of H3 from hairpin form to G-quadruplex with satisfactory results. All above findings manifested the biosensor can act as anticipated.

3.7. Properties analysis of the label-free electrochemical biosensor

In current-time curves of Figure 3A, the current signal gradually increase with the rising concentration (C) of guanine in the range of 5~100 nM with the regression equation $\Delta I = 5.965C + 47.82$ and the regression coefficient $r=0.9965$, where ΔI is the

current difference before and after the guanine addition. The biosensor possesses excellent sensitivity with the LOD down to 0.36 nM, which is 17~2000 folds lower than the existing methods (Table S1). Similarly, an analogous labeled electrochemical biosensor using methylene blue (MB) modified H4 as probe was built to challenge the sensitivity of our proposed label-free sensor. As shown in Scheme S1, the guanine triggered DGQ-to-quadruplex transformation may cause distance change of MB to the electrode surface as well as the electrochemical signal change for as low as 6 nM guanine detection (Figure S5). Therefore, our label-free sensor is more sensitive than the labeled one owing to the high specificity of hemin towards G-quadruplex and the signal amplification of the resulted DNAzyme, together with the signal-on strategy avoiding "false positive" caused by the contaminants in the reaction system. In Figure 3B, the ΔI generated by the guanine addition shows the highest column which is much higher than that of other analytes, including UTP, CTP, ATP, GTP, GDP, GMP, inosine, xanthosine, and analytes mixture, indicating higher selectivity of the biosensor. After measurement, the label-free electrochemical biosensor can be regenerated by incubating the used electrode in 88 °C aqueous solution for 5 min and then simple rinsing. Consequently, the current signal only decreased 8.4 % compared with previous response. In addition, after stored in buffer for 72 hours, the G-rich

DNA probe modified electrode showed 91 % of the previous current response, indicating its better stability.

3.8. The practical performance of the label-free electrochemical biosensor in real samples

Practically, we made use of this biosensor for acyclovir (Figure S6) detection to assess its practical performance in real samples. Acyclovir, a guanine derivative, is an antiviral medication (De Clercq and Field, 2006) which primarily applied as a cream or injection, and used for the treatment of herpes simplex virus infections, shingles and chickenpox (Awad and Cocchio, 2015). As shown in Figure 4, the current signals bear an excellent linear relationship with the concentration of standard acyclovir sample (it was purchased from China National Institute for the control of pharmaceutical and biological products) ranging from 10~100 nM with the LOD of 0.274 nM. Then, the biosensor was used for recovery test of acyclovir powder-injection (the batch number of the drugs produced by Hepu (Hubei) Pharmaceutical Co. Ltd. is 20160205, 20160301 and 20160709). Meanwhile, HPLC was used for comparison to evaluate the accuracy of the biosensor. As shown in Table S2, the recovery rates measured by our sensor ranging from 99 %~104 % were in a good accordance with that of HPLC. Moreover, because acyclovir excretes into urine by the

prototype drug in the main body metabolism process, the acyclovir-spiked urine samples derived from laboratory personnel without any preliminary treatment were also detected by the proposed biosensor above. As shown in Table S3, the average recoveries range from 96 % to 106 %, for low-, middle-, high concentration of acyclovir added into urine with the relative standard deviation (RSD) of 3.3 %~4.2 %. All above results demonstrate the better practicability and accuracy of our electrochemical biosensor.

4. Conclusion

In conclusion, two label-free biosensors (one is fluorescent and the other is electrochemical sensor) were developed for guanine and its derivatives detection with the LOD down to 18.26 and 0.36 nM, respectively. Owing to the extraordinary recognition ability of the defective G-quadruplex for guanine and ThT/ hemin against canonical G-quadruplex, the biosensors bear excellent selectivity. Moreover, the electrochemical biosensor also shows color changes of reaction solution regarding the concentration or existence of guanine, enabling visual detection by naked eyes. Finally, the label-free strategies not only reduce the background signal but also simplify the fabrication process and lower cost of the biosensors. All above

advantages make the proposed sensors possible being applied in diagnosis, treatment and inspection of diseases in the future.

Acknowledgement

The authors gratefully acknowledge the financial support of the National Science Foundation of Fujian Province (2017J07001, 2016J01042), United Fujian Provincial Health and Education Project for Tackling the Key Research .P.R. China (WKJ2016-2-30), Fujian Science and Technology Innovation Joint Found Project (2016Y9050).

References

Awad, N.I., Cocchio, C., 2015. Am. J. Health. Syst. Pharm. 72, 65-69.

Balagurumoorthy, P., Brahmachari, S.K., 1994. J. Biol. Chem. 269, 21858-21869.

Biffi, G., Tannahill, D., McCafferty, J., Balasubramanian, S., 2013. Nat. Chem. 5, 182-186.

Boss, G.R., Seegmiller, J.E., 1982. Annu Rev Genet. 16, 297–328.

Burge, S., Parkinson, G.N., Hazel, P., Todd, A.K., Neidle. S., 2006, Nucleic. Acids. Res. 34, 5402-5415.

Burhans, W.C., Weinberger, M., 2007. Nucleic. Acids. Res. 35, 7545-7556.

Cahours, X., Dessans, H., Morin, P., Dreux, M., Agrofoglio, L., 2000. J. Chromatogr. A. 895, 101-109.

Chabosseau, P., Buhagiar-Labarchède, G., Onclercq-Delic, R., Lambert, S., Debatisse, M., Brison, O., Amor-Guéret, M., 2011. Nat. Commun. 2, 368.

Chen, G., Chu, Q., Zhang, L., Ye, J., 2002. Anal. Chim. Acta. 457, 225-233.

Chen, J., Lin, J., Zhang, X., Cai, S., Wu, D., Li, C., Yang, S., Zhang, J., 2014. Anal. Chim. Acta. 817, 42-47.

Chen, S., Liu, P., Su, K., Li, X., Qin, Z., Xu, W., Chen, J., Li, C., Qiu, J., 2018. Biosens. Bioelectron. 99, 338-345.

Cui, Y., Yu, J., Feng, S., 2014. Talanta. 130, 536-541.

De Clercq, E., Field, H.J., 2006. Br. J. Pharmacol. 147, 1-11.

Fan, C., Plaxco, K.W., Heeger, A.J., 2003. Proc. Natl. Acad. Sci. U. S. A. 100, 9134-9137.

Fan, H., Li, S.P., Xiang, J.J., Lai, C.M., Yang, F.Q., Gao, J.L., Wang, Y.T., 2006. Anal. Chim. Acta. 567, 218-228.

Gao, F., Fan, T., Wu, J., Liu, S., Du, Y, Yao, Y., Zhou, F., Zhang, Y., Liao, X., Geng, D., 2017. Biosens. Bioelectron. 96, 62-67.

Hoogvliet, J.C., Dijksma, M., Kamp, B., van Bennekom, W.P., 2000. Anal. Chem. 72, 2016-2021.

Ito, Y., Hasuda, H., 2004. Biotechnol. Bioeng. 86, 72-77.

Jordheim, L.P., Durantel, D., Zoulim, F., Dumontet, C., 2013. Nat. Rev. Drug. Discov. 12, 447-464.

Kan, Z.Y., Yao, Y., Wang, P., Li, X.H., Hao, Y.H., Tan, Z., 2006. Angew. Chem. Int. Ed. Engl. 45, 1629-1632.

Kimura, T., Takeda, S., Sagiya, Y., Gotoh, M., Nakamura, Y., Arakawa, H., 2003. Nat. Genet. 34, 440-445.

Labib, M., Sargent, E.H., Kelley, S.O., 2016. Chem. Rev. 116, 9001-9090.

Li, L., Lu, Y.X., Ding, Y.P., Zhang, F.F., Wang, Y.P., 2012. Can. J. Chem. 90, 173-179.

Li, T., Li, B., Wang, E., Dong, S., 2009. Chem. Commun. 28, 3551-3553.

Li, X.M., Zheng, K.W., Hao, Y.H., Tan, Z., 2016. Angew. Chem. Int. Ed. Engl. 55, 13759-13764.

Li, X.M., Zheng, K.W., Zhang, J.Y., Liu, H.H., He, Y.D., Yuan, B.F., Hao, Y.H., Tan, Z., 2015. Proc. Natl. Acad. Sci. U. S. A. 112, 14581-14586.

Lu, S.H., Phang, R., Fang, J.M., 2016. Org. Lett. 18, 1724-1727.

Marchand, A., Gabelica, V., 2016. Nucleic. Acids. Res. 44, 10999-11012.

Marck, C., Thiele, D., 1978. Nucleic. Acids. Res. 5, 1017-1028.

Mohanty, J., Barooah, N., Dhamodharan, V., Harikrishna, S., Pradeepkumar, P.I., Bhasikuttan, A.C., 2013. J. Am. Chem. Soc. 135, 367-376.

Neves, S.R., Ram, P.T., Iyengar, R., 2002. Science. 296, 1636-1639.

Niu, X.L., Yang, W., Ren, J., Guo, H., Long, S.J., Chen, J.J., Gao, J.Z., 2012. Electrochim. Acta. 80, 346-353.

Pang, S.B., Zhang, Y., Wu, C.K., Feng, S.L., 2016. Sens. Actuators. B. Chem. 222,

857-863.

Pitceathly, R.D., Smith, C., Fratter, C., Alston, C.L., He, L., Craig, K., Blakely, E.L., Evans, J.C., Taylor, J., Shabbir, Z., Deschauer, M., Pohl, U., Roberts, M.E., Jackson, M.C., Halfpenny, C.A., Turnpenny, P.D., Lunt, P.W., Hanna, M.G., Schaefer, A.M., McFarland, R., Horvath, R., Chinnery, P.F., Turnbull, D.M., Poulton, J., Taylor, R.W., Gorman, G.S., 2012. Brain. 135, 3392-3403.

Shen, P., Xia, Y., 2014. Anal. Chem. 86, 5323-5329.

Sugimoto, S., Arita-Morioka, K., Mizunoe, Y., Yamanaka, K., Ogura, T., 2015. Nucleic. Acids. Res. 43, e92.

Tan, X., Wang, Y., Armitage, B.A., Bruchez, M.P., 2014. Anal. Chem. 86, 10864-10869.

Topkaya, S.N., Azimzadeh, M., Ozsoz, M., 2016. Electroanalysis. 28, 1-19.

Willner, I., Shlyahovsky, B., Zayats, M., Willner, B., 2008. Chem. Soc. Rev. 37, 1153-1165.

Wu, N., Lan, J., Yan, L., You, J., 2014. Chem. Commun. 50, 4438-4441.

Yoshimoto, K., Xu, C.Y., Nishizawa, S., Haga, T., Satake, H., Teramae, N., 2003. Chem. Commun. 24, 2960-2961.

Zhang, X., Wu, D., Liu, Z., Cai, S., Zhao, Y., Chen, M., Xia, Y., Li, C., Zhang, J., Chen, J., 2014. Chem. Commun. 50, 12375-12377.

Zhu, J., Zhang, L., Dong, S., Wang, E., 2015. Chem. Sci. 6, 4822-4827.

Scheme 1. A. The principle of the label-free fluorescent biosensor. B. The structural conversion of H1 before and after the addition of guanine.

Figure 1. The feasibility analysis of the label-free fluorescent biosensor. A. The fluorescent intensity of different solutions. a) ThT; b) ThT+H1; c) ThT+H1+K^+; d) ThT+H1+K^++G. B. The circular dichroism spectra of different solutions. a) K^++H1; b) K^++ H1+ThT; c) K^++ H1+G; d) K^++ H1+G+ThT. C. The UV-Vis spectra of different solutions. a) ThT; b) ThT+H1; c) ThT+H1+K^+; d) ThT+H1+K^++G. The concentrations of K^+, ThT, H1 and G were 10 mM, 5 μM, 50 nM and 10 μM, respectively.

Figure 2. Properties analysis of the label-free fluorescent biosensor. A. The fluorescent intensity of different concentration guanine (a→k, μM: 0, 0.05, 0.1, 0.5, 1, 5, 10, 20, 30, 40, 50) on the label-free fluorescent DNA biosensor. Inset: Linear regression curve and equation of the change of fluorescence intensity (ΔF) after the addition of the analytes versus guanine concentration (C). B. The fluorescence intensity of the biosensor (a, the blank) with addition of 10 μM guanine (k), UTP (b), CTP (c), ATP(d), Inosine (e), Xanthosine (f), GTP (g), GDP (h), GMP(i) and Mix (j, the mixture of all above analogues and each analogue in the Mix is 10 μM too),

respectively. Inset: The change of fluorescence intensity (ΔF) after the addition of the analytes. C. The discrimination factor (DF) comparison of the label-free (blue rectangle) and labeled (red rectangle) fluorescence biosensors. $DF=\Delta F_{guanine}/\Delta F_{analogue}$.

Scheme 2. A. The principle of the label-free electrochemical biosensor. B. The cyclic voltammograms of different electrodes in TMB-H_2O_2 solution. a) K^++H3; b) K^++ hemin; c) K^++H3+G; d) K^++H3+hemin; e) K^++H3+G+hemin. The concentrations of K^+, hemin, H3 and guanine were 5 mM, 5 μM, 50 nM, 10 μM, respectively.

Figure 3. The properties analysis of the label-free electrochemical biosensor. A. The current-time curves of different concentrations of guanine on the label-free electrochemical biosensor. (a→g, nM): 0, 5, 20, 40, 60, 80, 100. Inset is the linear regression curves and equations of ΔI and C. B. The change values of current intensity of the biosensor with addition of 100 nM guanine, UTP, CTP, ATP, Inosine, Xanthosine, GTP, GDP, GMP and Mix (the mixture of all above analogues and each analogue in the Mix is 100 nM too), respectively.

Inset is the linear regression curves and equations of ΔI and C. B. The change values of current intensity in the same concentration of guanine, UTP, CTP, ATP, Inosine, Xanthosine, GTP, GDP, GMP and Mix.

Figure 4. The current-time curves of different concentrations (a→g, nM: 0, 10, 20, 40, 60, 80, 100) acyclovir on the label-free electrochemical biosensor. Inset: Linear regression curves and equations for ΔI and C.

Figures:

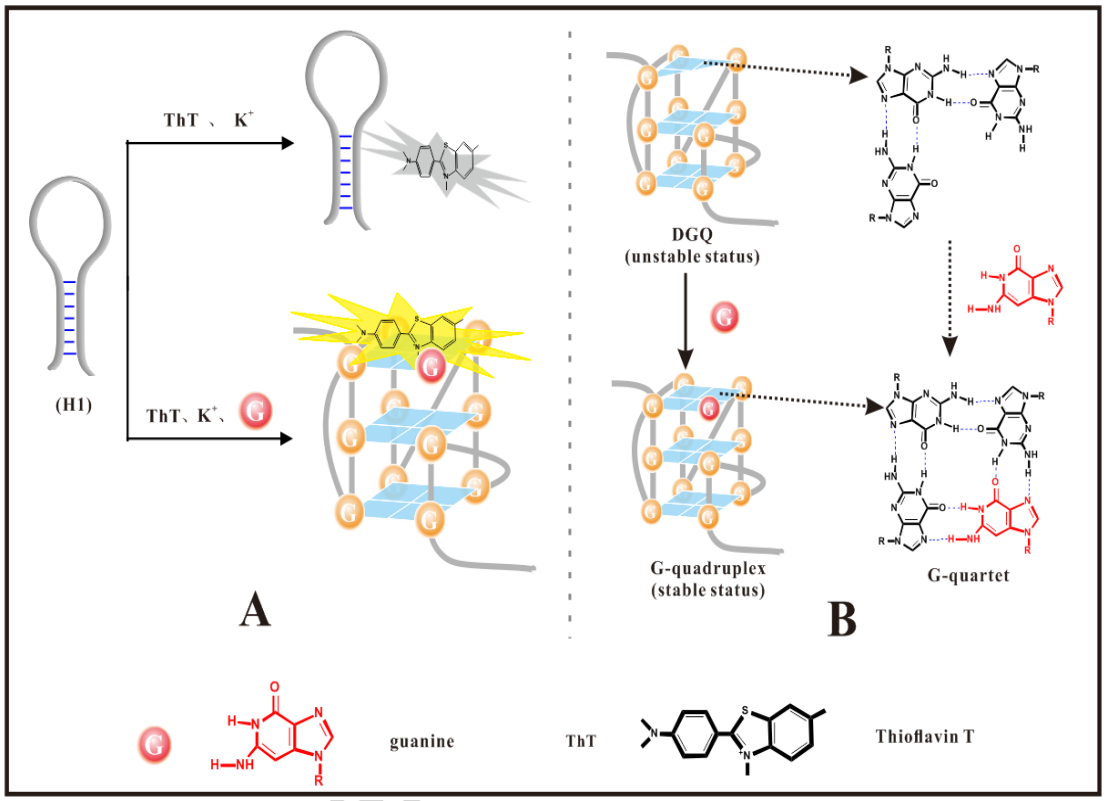

Scheme 1

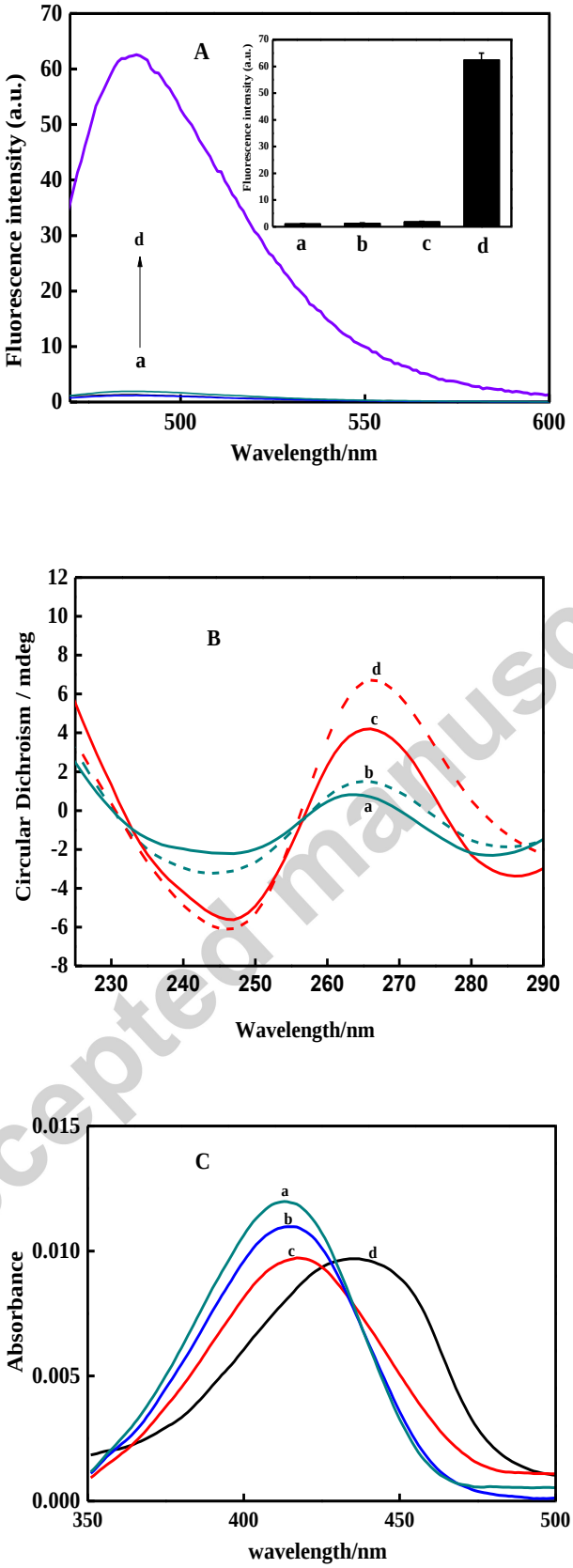

Figure 1

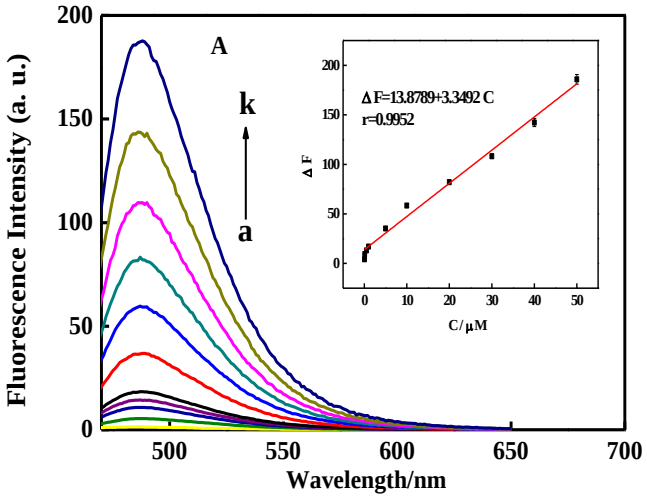
A
k
a
Fluorescence Intensity (a. u.)
Wavelength/nm
ΔF=13.8789+3.3492 C
r=0.9952
Δ F
C/μM

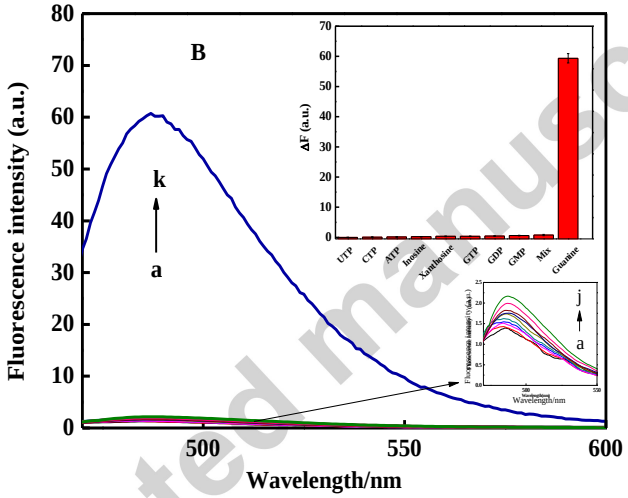
B
k
a
Fluorescence intensity (a.u.)
Wavelength/nm
ΔF (a.u.)
UTP
CTP
ATP
Inosine
Xanthosine
GTP
GDP
GMP
Mix
Guanine
j
a

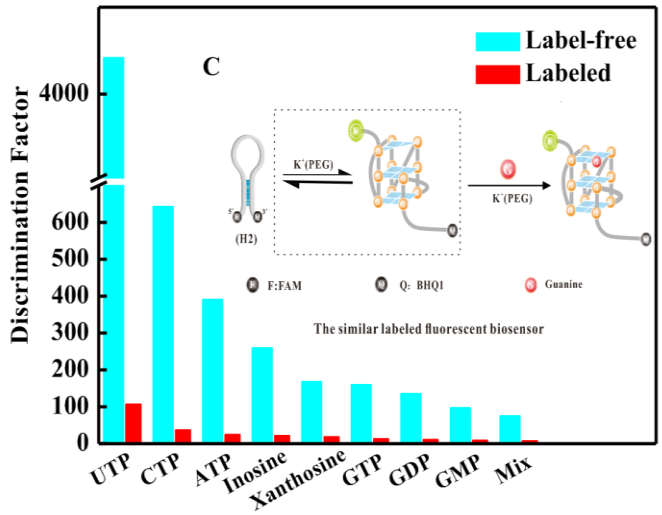
C
Label-free
Labeled
Discrimination Factor
K+(PEG)
(H2)
F:FAM
Q: BHQ1
Guanine
The similar labeled fluorescent biosensor
UTP
CTP
ATP
Inosine
Xanthosine
GTP
GDP
GMP
Mix

Figure 2

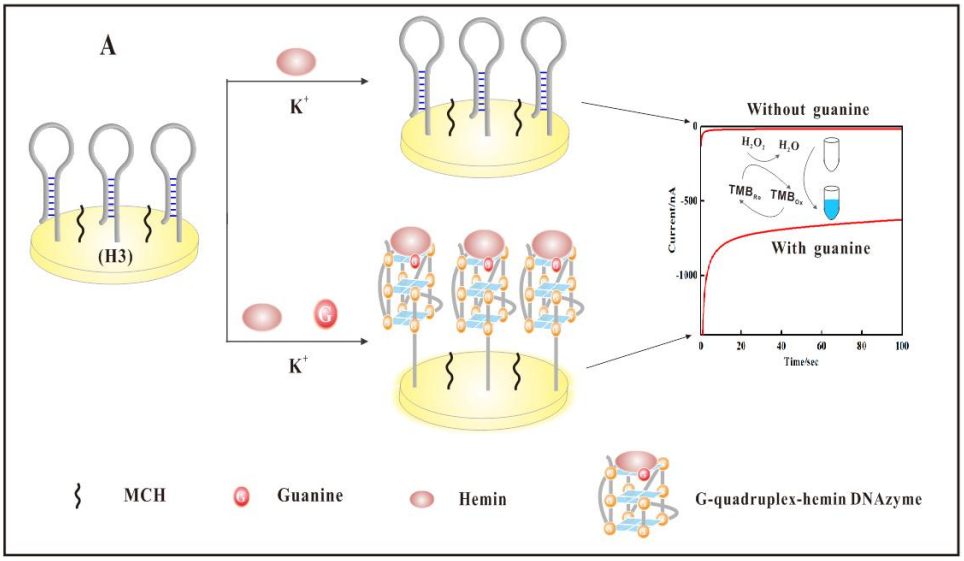

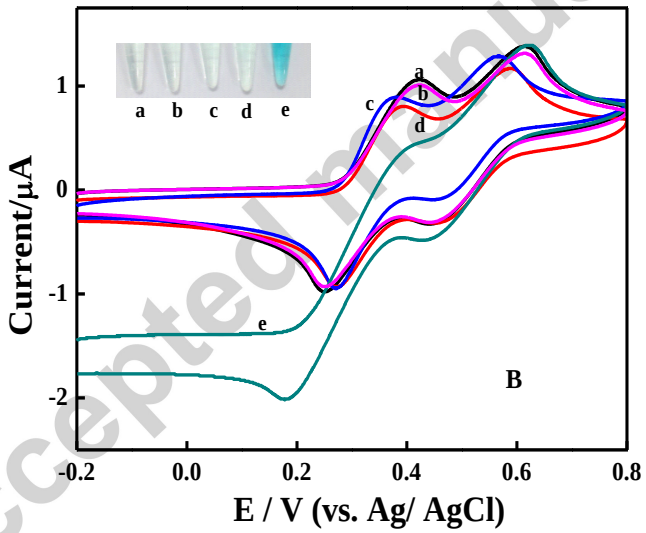

Scheme 2

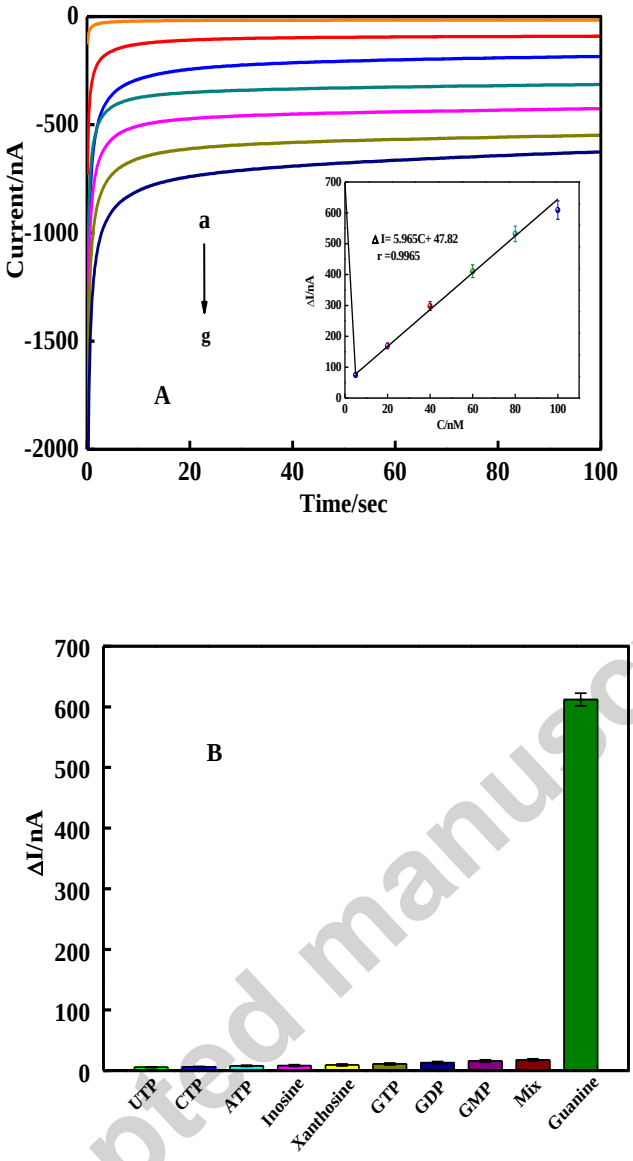

Figure 3

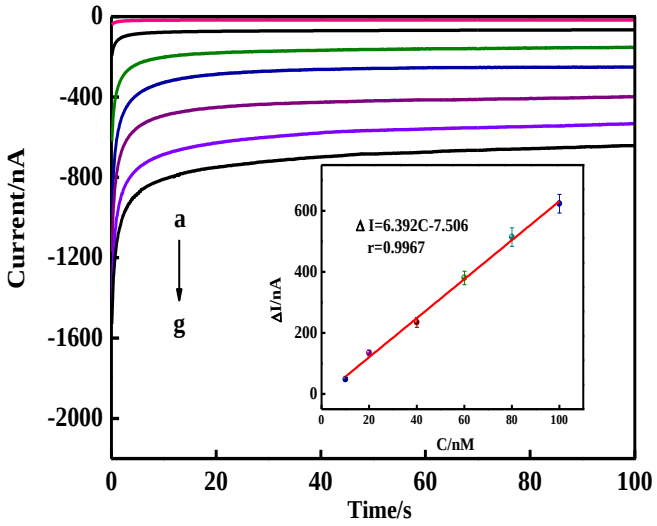

Figure 4

Highlights:

1. A fluorescent and an electrochemical biosensor were developed based on defective G-quadruplex and ThT/hemin.

2. The unique recognition of the defective G-quadruplex for guanine confers excellent properties to the proposed biosensors.

3. The perfect discriminative ability of ThT and hemin against canonical G-quadruplex further increase the sensor's performance.